RSC Advances

ROYAL SOCIETY OF CHEMISTRY

www.rsc.org/advances

Nanoincorporation of Curcumin in Polymer-Glycerosomes and Evaluation of their *In Vitro-In Vivo* Suitability as Pulmonary Delivery Systems

Maria Letizia Manca[1], José E. Peris[2*], Virginia Melis[2], Donatella Valenti[1], Maria Cristina Cardia[1], Donatella Lattuada[3], Elvira Escribano-Ferrer[4], Anna Maria Fadda[1], Maria Manconi[1]

[1] Department Scienzedella Vita e dell'Ambiente, CNBS, University of Cagliari, Cagliari, Italy.

[2]Department of Pharmacy and Pharmaceutical Technology, University of Valencia, Burjassot, Valencia 46100, Spain

[3]Departament of Medical Biotechnologies and Translational Medicine, University of Milan, Milan, Italy

[4]Department of Pharmacy and Pharmaceutical Technology, School of Pharmacy. Institute of Nanoscience and Nanotechnology, University of Barcelona, Barcelona, Spain

* Corresponding author: José-Esteban Peris

Tel.: +34 96 3543353; fax: +34 96 3544911

E-mail address: jose.e.peris@uv.es

Abstract

The aim of this work was to deliver the curcumin to lungs by its incorporation into innovative vesicles obtained using phospholipids and high concentrations of glycerol (50%, v/v), so called glycerosomes, and combining them with two polymers: sodium hyaluronate and trimethyl chitosan to obtain polymer-glycerosomes. These systems were prepared avoiding organic solvents or acidic solutions and their physico-chemical properties were fully characterized. Cryogenic transmission electron microscopy and small-angle X-ray scattering showed that both glycerosomes and polymer-glycerosomes were spherical, mainly unilamellar with nanometric size (65-112 nm). Vesicles showed a good aptitude to be nebulized being the largest amount of curcumin found in the latest stages of a Next Generation Impactor™. *In vitro* results revealed the high biocompatibility of samples especially those containing the polymers. Curcumin loaded vesicles were also able to protect *in vitro* A549 cells stressed with hydrogen peroxide, restoring the healthy conditions, not only by directly scavenging free radicals but also indirectly inhibiting the cytokine IL6 and IL8 production. Moreover, *in vivo* results in rats showed the high capacity of these formulations to favour the curcumin accumulation in the lungs confirming their potential use as a target system for the treatment of pulmonary diseases.

Keywords: hydrophilic polymers, glycerol, oxidative stress, IL6 and IL8 cytokines, In-Vivo FX PRO Imaging System

Introduction

Local pulmonary disorders such as asthma, bronchitis, cystic fibrosis and chronic obstructive pulmonary disease are heterogeneous disorders generally characterized by common symptoms: airway inflammation, fibrosis, mucus plugging and emphysema. Infiltration of inflammatory cytokines, oxidative stress and chronic inflammation are the pathological conditions associated to the development and progression of these diseases. For this reason, a treatment with drugs having antioxidant and anti-inflammatory properties may be beneficial in preventing or slowing the progression of these disorders. Several plant-derived secondary metabolites are capable of directly affect inflammatory mediators, as well as production and activity of second messengers, transcription factors and pro-inflammatory molecules expression inhibiting consequent pathological conditions [1,2]. Polyphenols, such as flavonoids, are known as potent antioxidants and antiinflammatory and, among all, curcumin exhibits a wide range of pharmacological activities against many chronic diseases including type II diabetes, rheumatoid arthritis, multiple sclerosis, Alzheimer's disease and atherosclerosis [3–7]. Further studies disclosed the curcumin ability to enhance wound healing [8] and protect against liver and pulmonary injury or fibrosis [9–11]. Additionally, curcumin not only inhibits tumor cell proliferation and metastasis, but also induces their apoptosis by modulating several pro-inflammatory factors (e.g. interleukin IL1, IL1b, IL12), tumor necrosis factor α (TNF-α) and interferon γ (INF-γ) [12]. In spite of its potential activity, curcumin bioavailability is limited by its very low aqueous solubility (0.6 mg/ml) and its susceptibility to degradation, especially under alkaline conditions [13]. Indeed, its pulmonary delivery may represent a valid alternative; however, an appropriate vehicle is required because in water curcumin may aggregate in large particles affecting the atomization and homogeneous distribution of aerosol inhaled droplets. A possible strategy to improve curcumin pulmonary delivery is its loading into suitable nanocarriers, able to ameliorate drug aerosol performances and local tissue deposition and distribution. Among others, liposomes, versatile systems able to load

both lipophilic and hydrophilic compounds, have been widely used as drug delivery systems as well as for pulmonary delivery of active compounds because they are safe and biocompatible. Although, the use of liposomes as pulmonary delivery systems give encouraging results, their nebulization may be ameliorate by addition of other components [14–18]. Indeed, their composition has been differently modified, also using polymers, which were aspect to improve the vesicle stability during atomization and their homogeneous distribution in the deeper airway. For the best of the knowledge, in this work a new kind of phospholipid vesicles, called polymer-glycerosomes, were used for the first time as lung delivery systems in an attempt to improve the local deposition of a low bioavailable natural compound, curcumin. These systems were based on phospholipids and high concentrations of glycerol (50%, v/v), and their performances were further modified by the addition of two different hydrophilic polymers: sodium hyaluronate and trimethyl chitosan. Vesicle main components were phospholipids and glycerol, two harmless and fully accepted compounds for different types of pharmaceutical administrations. In previous works, glycerosomes were prepared and tested as skin delivery systems of natural and synthetic compounds [19,20]. In the present work, the addition of the polymers to the vesicles allowed to obtain them using an organic solvent-free and environmentally-friendly method previously proposed to obtain hyalurosomes [8].

Hyaluronic acid is a natural, biocompatible and biodegradable polysaccharide that is distributed widely throughout the human body, mainly in the connective tissue, eyes, intestine and lungs where is mainly metabolize by hyaluronidase [21]. In addition hyaluronic acid plays an important role in the function of various inflammatory mediators and have beneficial effects on the mucociliary transport rate in airways, due to the mucoadhesivity of the polymer [22–25]. Thanks to its endogenous origin, easy degradation, elastic-viscous properties and stabilizing ability, it is often added to phospholipid vesicle formulation intended for lung delivery [26,27]. Due to its high water solubility, it is widely used in pharmaceutical formulations as sodium salt, which was used in the present study, to prepare hyaluronan-glycerosomes (HY-glycerosomes).

The chitosan choice was related to its favourable and versatile properties that make it as an attractive option for designing adequate and advanced lung delivery systems. In fact, it is a polymer highly biocompatible, biodegradable and mucoadhesive; moreover, possesses antimicrobial and antioxidant properties potentially useful for the development of pulmonary delivery systems [28]. Despite its pharmaceutical suitability, chitosan has a limited aqueous solubility (only at pH<5.6) and many efforts have been made to increase its water solubility especially at neutral and basic pH values, by modifying its structure [29]. Trimethyl chitosan is an example, and its use in pharmaceutical nanoformulations is promising [30,31]. In the present work, trimethyl chitosan chloride was synthesized and used to obtain trimethyl chitosan-glycerosomes (TMC-glycerosomes). The purpose of the present work was to obtain new hyaluronan- or trimethyl chitosan-glycerol/phospholipid vesicles, combining the innovative composition of glycerosomes with the environmentally friendly technology previously used to prepare hyalurosomes and to test, for the first time, these polymer-glycerosomes as lung delivery systems for curcumin. In order to this, i) curcumin loaded glycerosomes, HY-glycerosomes and TMC-glycerosomes were formulated and characterized; ii) the *in vitro* aerodynamic behaviour of the formulations were evaluated by means of the Next Generation Impactor^{TM}; iii) the *in vitro* biocompatibility, antioxidant and anti-inflammatory effects of curcumin loaded vesicles were assessed on pulmonary epithelial cells (A549); and iiii) the *in vivo* curcumin lung accumulation were studied after intratracheal administration of formulations, in rats.

2. Results

2.1. Synthesis and characterization of trimethyl chitosan chloride

The water soluble, trimethyl chitosan chloride, was synthesised and the degree of quaternization, determined by ^{1}H-NMR spectroscopy using the procedure of water suppression, was ~70%. The obtained polymer was soluble in water at the used concentration of 0.1% (w/v).

2.2. Preparation and characterization of vesicles

Taking into account the results obtained in a previous work [20], which underline that high amount of glycerol better improve the characteristics of quercetin loaded glycerosomes, a preformulation study was carried out using the same phospholipid amount (180 mg/ml) and hydrating them by direct addition of the water dispersion of curcumin (2 mg/ml; to obtain liposomes) or the glycerol/water mixture (30 or 50% v/v) to obtain glycerosomes. The liposome dispersion was very turbid like an emulsion, the vesicles were large (size ND), high polydispersed and the curcumin precipitated after immediately the preparation, 30%glycerosome dispersion was turbid as well, vesicles were smaller but the curcumin precipitated after the preparation. Differently, curcumin (2 mg/ml) was stably incorporated in 50%glycerosomes resulting in a yellow-opalescent and high viscous dispersion (Figure 1A). Then, 50% (v/v) of glycerol was selected as suitable concentration to perform the study and this formulation was used as phospholipid-base formulation (reference). Curcumin loaded polymer-glycerosomes were prepared by direct hydration of phospholipids with drug/polymer/glycerol/water mixtures avoiding the use of organic solvents. Probably, glycerol and polymers together facilitate the curcumin homogenous dispersion and/or its partially solubilisation [32] and the resulting polymer-glycerosomes gave rise a very fluid, yellow and transparent colloidal dispersion (Figure 1B and 1C). Cryo-TEM observation of vesicles confirmed the presence of spherical and regular vesicles, mainly unilamellar, except for TMC-glycerosomes, which partially formed oligolamellar structures (Figure 1).

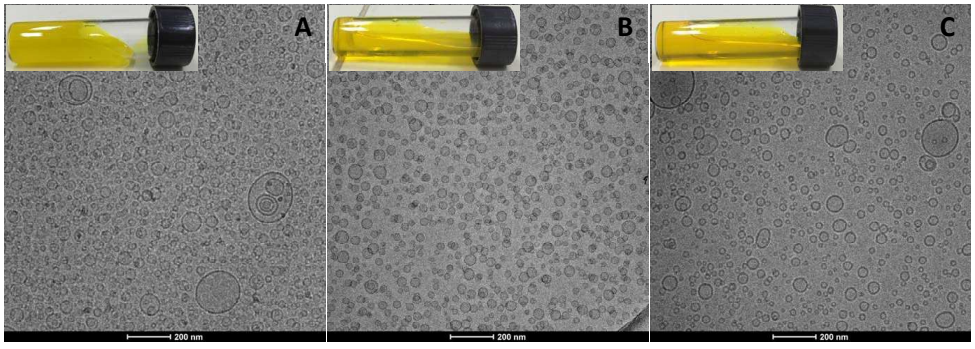

Dynamic laser light scattering measurements (Table 1) showed that glycerosomes had the smallest mean diameter (~62 nm, $p<0.05$ versus all) in a fairly homogeneous system (P.I.=0.28), while HY-

glycerosomes and TMC-glycerosomes were larger (~80 and 112 nm, $p<0.05$ between all) with a higher polydispersity index (P.I. ≥0.33, $p<0.05$ versus glycerosomes).

Table 1: Mean diameter (MD), polydispersity index (P.I.), zeta potential (ZP), entrapment efficiency (EE), and aggregation efficiency (AE) of curcumin (CUR) loaded glycerosomes, HY-glycerosomes and TMC-glycerosomes. Mean values ± standard deviations (SD) were obtained from at least 6 independent samples. The same symbols indicate values statistical equivalents ($p>0.05$).

	Size±SD (nm)	**P.I.**	**ZP±SD (mV)**	**EE±SD (%)**	**AE±SD (%)**
Glycerosomes	°62±4	*0.28	*-52±2	*74±4	*91±3
HY-glycerosomes	*80±2	°0.32	*-56±5	*74±2	*87±4
TMC-glycerosomes	"112±6	°0.34	°-43±2	*73±2	*93±2

The zeta potential of formulations was highly negative (~ -50 mV), predicting a great stability of the dispersions. The surface charge of all vesicles was negative mainly because P90G is a mixture of phosphatidylcholine, other phospholipids and fatty acids. Being phosphatidylcholine a zwitterionic molecule, the orientation and conformation of its headgroup is not constant and can be influenced by binding or adsorption of the negatively charged molecule as well sodium hyaluronate, which can interact with choline groups on the both bilayer surfaces forming a structured vesicle-polymer system [8]. TMC-glycerosomes showed a less negative zeta potential (-43 mV, $p<0.05$ versus others) as a consequence of the partial neutralization of phosphatidylcholine negative groups by the positive charges of trimethyl chitosan.

The curcumin concentration after preparation was checked by HPLC and the calculated amount corresponded to the amount initially used (~2 mg/ml) in all the formulations. Both glycerosomes and polymer-glycerosomes were able to incorporate high amounts of curcumin (~74%, $p>0.05$

among groups), the great part of the used phospholipids were aggregated to form vesicles (AE%~90%, p>0.05 among groups) and both parameters did not seem to be affected by the presence of polymers which did not hamper drug incorporation and vesicle formation. The vesicle stability was evaluated monitoring their physico-chemical characteristics during a storage period of 90 days at room temperature (Figure 2).

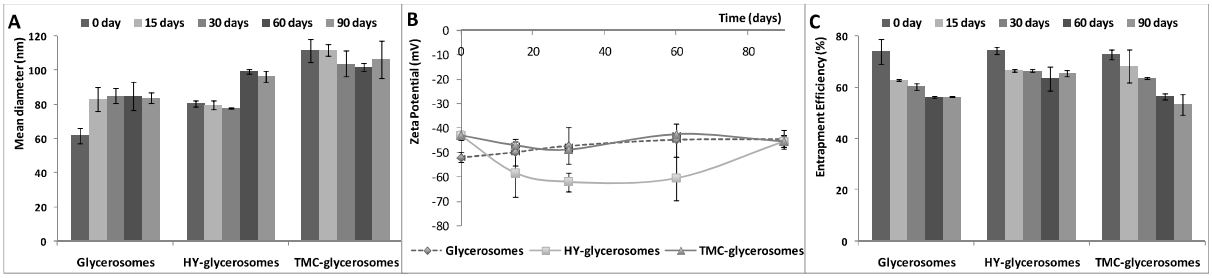

Mean diameter of glycerosomes (which were the smallest vesicles) increased up to ~80 nm ($p<0.05$ versus the initial value) after 30 days and then remained constant until 90 days of storage. HY-glycerosomes only increased in size (fom ~80 to ~100 nm, $p<0.05$ versus the initial value) after 60 days, whereas TMC-glycerosomes, which were the largest vesicles, kept their size ($p>0.05$) during the storage period (Figure 2A). Zeta potential of all the formulations tested remained unchanged while the entrapment efficiency decreased during 90 days of storage, mainly that of glycerosomes and TMC-glycerosomes which diminished up to ~55% ($p<0.05$ versus the initial values and HY-glycerosome value at 90 days). Entrapment efficiency of HY-glycerosomes underwent only an initial reduction (~10%, $p<0.05$ versus start value) and then remained constant.

2.3. Small-Angle X-ray Scattering

SAXS pattern confirmed the cryo-TEM results. In fact the peak of glycerosomes and HY-glycerosome was a first order, broaden and unsharpened peak denoting well defined unilamellar vesicles while TMC-glycerosome peak was asymmetric and showed a lateral hump probably due to the presence of low-lamellar vesicles. The parameters of vesicle bilayer calculated according to Pabst model [33] confirmed the effective formation of lamellar vesicles, liposome like, that was not modified by the polymer addition. Vesicle structure was very similar as well as the main parameters

like bilayer thickness (d_B) ~46 Å, polar head amplitude (σ_H) ~2.8 Å, and distance of head group from the center of the bilayer (Z_H) ~17.4 Å (Figure 3). SAXS patterns of empty vesicles (data not shown) were very similar to that of curcumin loaded vesicles.

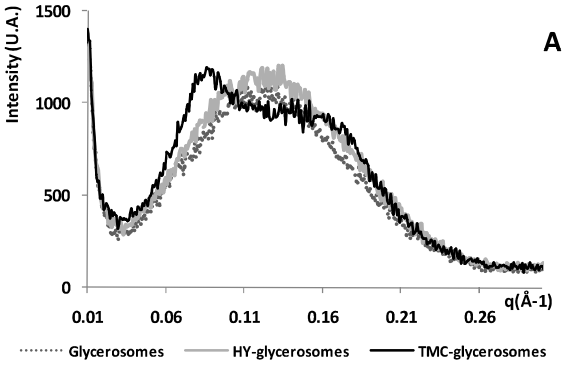

A

B	z_H (Å)	σ_H (Å)	d_B (Å)
Glycerosomes	17.6±0.2	2.7±0.2	46±1
HY-glycerosomes	17.5±0.2	2.6±0.2	45±1
TMC-glycerosomes	17.0±0.6	3.1±0.5	47±3

2.4. Aerodynamic properties of samples

Formulations were sprayed using the PariSX® air jet nebulizer connected to the NGI, and the drug deposition and the aerodynamic diameter of each formulation was evaluated. Nebulization was performed for 15 min, which was appropriate to combine both patient compliance and nebulisation of a great amount of vesicular dispersion. For each formulation the nebulizer content was not completely aerosolized being the Emitted Dose (ED%) always lower than 100%: ~43% for glycerosomes and ~55% for polymer glycerosomes. Assessment of the aerodynamic parameters (Table 2) revealed that MMAD was always lower than 5 μm:~ 4.4 μm for glycerosomes and smaller for both polymer-glycerosomes (~3.6 μm, $p<0.05$ versus glycerosomes), proving that the droplets formed during the aerosolization process may reach the lungs. FPF was ~60% for all formulations ($p>0.05$) confirming that more than 59% of aerosolized droplets were sized below 5 μm and could potentially reach the deep lungs.

Table 2. Fine particle dose (FPD), fine particle fraction (FPF) and mass median aerodynamic diameter (MMAD) of curcumin formulations using the Next Generation Impactor. All values are

shown as mean ± standard deviation of three experiments, while MMAD values are reported as mean ± geometric standard deviation. The same symbols indicate values statistically equivalents ($p>0.05$).

	FPD (mg)	FPF (%)	MMAD
Glycerosomes	0.46±0.07	*60±2	4.5±0.6
HY-glycerosomes	*0.64±0.04	*61±4	*3.6±0.3
TMC-glycerosomes	*0.57±0.09	*58±5	*3.7±0.5

The percentage of curcumin deposited in each stage of the impactor as a function of droplet size was very similar for all the formulations (Figure 4A) and no real impact of the polymers could be observed: ~55% of curcumin was contained in droplets ranging from 5.39 to 0.98 μm (stages 3-7). The mean diameter of vesicles recovered in each stage of the impactor was measured to evaluate their stability during the process (Figure 4B).

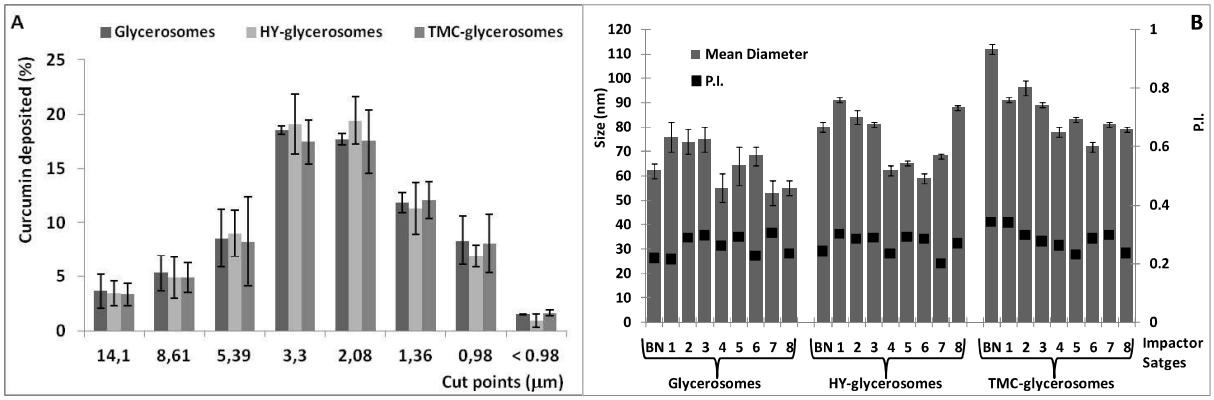

The mean diameter of glycerosomes deposited in the first three stages was ~75 nm, only slightly higher than the initial size (62 nm, $p<0.05$) and decreased up to ~57 nm ($p<0.05$ versus 75) in the next stages (4-8). Polymer-glycerosomes showed a similar behaviour, size was larger, ~89 nm in the initial stages (3) and subsequently decreased up to ~70 nm ($p<0.05$ versus 89) in the others stages. Results indicated that, destabilizing forces involved during the nebulization process, caused only a small variation of vesicle size and P.I. but did not induce vesicle aggregation in large

particles and the consequent drug leakage. Overall, *in vitro* nebulization results demonstrated a fairly good aptitude of the three formulations to be nebulized, which can be predictive of the improvement of curcumin deposition in the lung.

2.5. *In vitro* cytotoxicity, antioxidant and anti-inflammatory activity of curcumin-loaded vesicles, on A549 cells

Despite the well-known safety of all the used components (i.e. phospholipids, hyaluronic acid, trimetyl chitosan and curcumin), cytotoxicity of curcumin loaded vesicles was checked, as a function of curcumin concentration, (Figure 5A) and compared with that of curcumin dispersion. The viability of cells incubated with curcumin dispersion was the lowest (~80%) without statistical differences ($p>0.05$) among the different dilutions. When cells were treated with vesicles at the lowest dilution (curcumin 40 µg/ml) the same viability provided by dispersion (~82%, $p>0.05$) was obtained, regardless the formulation used. Using glycerosomes at higher dilutions (curcumin 20, 10, 4 and 2 µg/ml) the viability slight increased (~89%, $p>0.05$) being higher, but not statistically different, than that obtained using the dispersion ($p>0.05$). Incubation with HY-glycerosomes (except at the lowest dilution, 40 µg/ml of curcumin) allowed to improve the cell viability respect to curcumin dispersion (always ≥100%), in particular at the highest three dilutions (~113%, $p<0.05$). TMC-glycerosomes increased in a lesser extend the cell viability (~99%, $p<0.05$) respect to curcumin dispersion (except at the lowest dilution). Results underlined that the curcumin incorporation in vesicles, especially in polymer-glycerosomes, ameliorate the drug biocompatibility especially when they were used at a concentration of 20 µg/ml of curcumin which was used for further study.

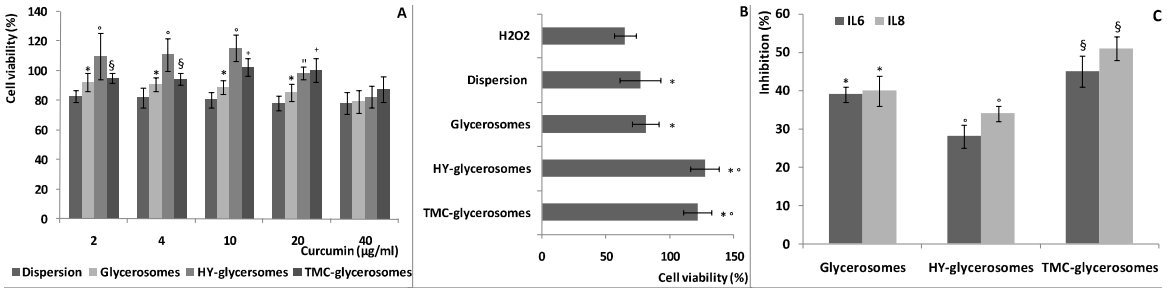

The short-term (6 h) protective effect of curcumin formulations, against the oxidative stress induced *in vitro* on A549 cells by H_2O_2 was also evaluated (Figure 5B). The H_2O_2 treatment reduced the cell viability up to 60% (positive control) and all curcumin formulations exerted a restoring effect ($p<0.05$ versus positive control) reducing the cell mortality. The protective effect of curcumin was slightly evident using its water dispersion and glycerosomes (~ 80% viability, $p<0.05$ versus positive control) and was especially reinforced by its incorporation into HY- and TMC-glycerosomes which totally counteracted the damaging effect of H_2O_2 and additionally allowed cell proliferation up to ~120% of viability. HY- and TMC-glycerosomes seem to facilitate cellular uptake of curcumin which may exert its scavenging activity in the intracellular environment, thus, preventing cell damages and consequent death.

The ability of curcumin loaded vesicles to down regulate the production of two pro-inflammatory cytokines IL-6 and IL-8 was evaluated on a *in vitro* long-time study (4 days) using A549 cells. Cytokine expression was measured by FACS analysis (Figure 5C). All formulations significantly inhibited the production of both IL6 and IL8 in comparison with untreated cells (control, $p<0.05$). Curcumin loaded TMC-glycerosomes was the most effective formulation able to inhibit the secretion of both cytokines reaching ~52%, while the efficacy of HY-glycerosomes was lower ~22%, $p<0.01$.

2.6. *In vivo* biodistribution studies

In vivo biodistribution studies were performed by intratracheal administration of curcumin dispersion and curcumin loaded vesicles to rats, measuring the plasma concentration of drug and its retention in the trachea, lungs and liver. During the 24 h experiment, curcumin was not detected in plasma or its concentration was below the limit of quantification, confirming its low systemic distribution and its reduced accumulation in non-targeted tissues. All formulations improved the total drug deposition in the whole lungs at 24 h respect to the curcumin dispersion (used as control, $p<0.05$) following the ranking: HY-glycerosomes>TMC-glycerosomes>glycerosomes>control (Figure 6A). HY-glycerosomes gave the same drug deposition in the trachea and in each lobe of the

lungs (~0.75 µg/g, p>0.05 among groups), except in the right inferior lobe in which the amount was slightly higher (~0.85 µg/g, p<0.05). TMC-glycerosomes provided a homogeneous distribution of curcumin (~0.68 µg/g) in the trachea and the three lung lobes, the amount of curcumin was slightly lower only in the residual lung (~0.45 µg/g, p<0.05). Using glycerosomes, the amount of drug accumulated in each lobe of lungs and trachea was homogeneous (~0.37 µg/g) but values were not statistical different than that found using the control (p>0.05). For all tested formulations the amount of the drug found in the liver was ≤0.004 µg/g confirming the negligible accumulation in non-targeted tissues. As confirmation of previous findings fluorescent curcumin accumulation in the lung was visualized using the In Vivo FX PRO Imaging System (Figure 6B).

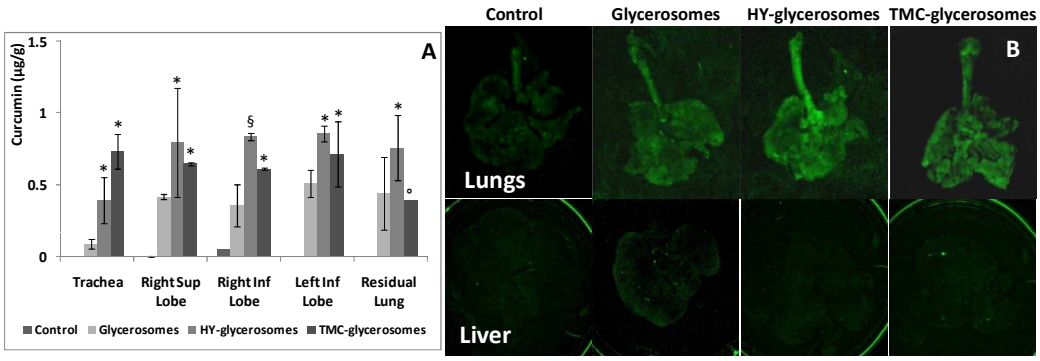

Following treatment with all the vesicles, a higher fluorescence than that of control was detected in the lungs. In particular lungs treated with HY-glycerosomes showed the highest fluorescence. The fluorescence intensity of lungs treated with TMC-glycerosomes was slightly lower while those treated with glycerosomes showed the weakest fluorescence. In the liver a slight fluorescence was detected using glycerosomes, showing their lower selectivity for lungs respect to polymer-glycerosomes, which on the contrary, provided a high affinity for pulmonary tissues and any liver or systemic distribution was detected, confirming their potential use as a targeting system for the lungs.

3. Discussion

Considering the promising performances provided by glycerosomes in skin delivery, here their innovative composition was combined with the environmentally-friendly technology of

hyalurosomes to obtain polymer-glycerosomes [8,19,34,35]. These new vesicles were tested for the first time as carriers for pulmonary delivery of curcumin and their performances were compared with that of conventional glycerosomes used as reference due to the impossibility to have the corresponding conventional liposomes. In the preformulation study, the mixture glycerol/water 50% v/v was selected as the most suitable to obtain curcumin loaded glycerosomes. The polymer was initially dispersed with the curcumin in the glycerol/water mixture facilitating the curcumin stabilization in the polymeric network and probably its partial solubilisation as previously reported for Eudragit/curcumin dispersion [32]. The obtained homogenous and transparent dispersions were used as hydration medium of phospholipids, facilitating HY-glycerosome assembling and stabilization.

The partial substitution of amino hydrogen with methyl groups converted chitosan in the water soluble trimethyl chitosan which allowed to obtain TMC-glycerosomes using the same biocompatible procedure applied for HY-glycerosomes and avoiding the use of acidic solution usually needed to solubilise chitosan [8,36]. The safety of a drug delivery system is particular crucial for pulmonary formulations. For this reason, natural and well-known safe components were used to prepare the tested vesicles (i.e. phospholipids, sodium hyaluronate and trimetyl chitosan) and their biocompatibility with human lung epithelial cells was confirmed, especially that of HY-glycerosomes, which at concentrations of curcumin ranging from 20 to 2 μg/ml improved cell viability up to ~108% probably due to the proliferative effect of hyaluronan [37]. By virtue of its natural origin and polyfunctional properties, curcumin appears to be an ideal agent to treat inflammatory and oxidative stress conditions in the lungs [38]. Indeed, it can directly avoid oxidative stress scavenging superoxide, hydroxyl radical and nitric oxide free radicals [39] and indirectly down regulate the expression of multifunctional proinflammatory cytokines (i.e. IL-6 and IL-8) actively involved in the endogenous oxidative stress, inflammation and carcinogenesis [40]. In this work, these helpful curcumin properties were confirmed and its antioxidant activity *in vitro* was improved by its inclusion in polymer-glycerosomes. In particular, the endogenous production of oxidative and

inflammatory mediators was greatly inhibited by TMC-glycerosomes. Additionally, the incorporation of the active into glycerosomes and polymer-glycerosomes provided a good curcumin nebulization *in vitro* overcoming its limited water solubility, which make difficult to achieve therapeutic concentrations in lungs. In fact, jet nebulization method involves repeated cycles of aerosol droplet formation and their recapture in the nebulizer reservoir before the formulation leaves the device. Previously findings disclosed that the considerable shearing forces applied during the nebulization, facilitated the solvent elimination and the formation of large drug aggregates unable to reach the last part of the respiratory tract or to go away the device. The combination of the nanotechnologies, the innovative preparation method and the employment of glycerosomes seems to overcome these drawbacks permitting curcumin to stay inside the vesicles, which can reach intact the last stages of the impactor probably thanks to their high resistance to the shearing forces [41]. This vesicle resistance seemed to be independent from their composition probably because the structure and size of vesicles were very similar, simply TMC-glycerosomes were oligolamellar and consequently slightly larger than glycerosomes and HY-glycerosomes which were unilamellar and smaller. The deposition in lung epithelia of curcumin still loaded in vesicles and not as free drug represents an important advantage due to the well-known ability of phospholipid vesicles to facilitate the drug passage through biological membranes overcoming the barrier formed by the lung epithelial cells that prevents the absorption of inhaled substances [42].

Despite to the comparable physico-chemical properties of vesicles and their *in vitro* aerosolization performances, the *in vivo* biodistribution study underlined a superior ability of both HY- and TMC-glycerosomes respect to glycerosomes as lung delivery system disclosing that the addition of both polymers to glycerosomes improved the *in vivo* curcumin accumulation. This could be explained because the polymer acted as key component forming less viscous dispersions and favouring the vesicle adhesiveness and deposition in the lung tissue. Additionally, these carriers were able to maximize the *in vitro* curcumin protective effect against the oxidative stress on lung cells and

provided an optimal inhibition of proinflammatory cytokine production indeed it is expected to exert the same activity *in vivo* after their deposition in the lungs.

4. Conclusions

During this study, the new plymer-glycerosome formulations were tailored using the hyalurosome method for their preparation to deliver the curcumin in lungs. Then, HY- and TMC-glycerosomes were obtained in one-step method only using phospholipids, glycerol, polymers, curcumin and water. Overall *in vitro* and *in vivo* outcomes highlighted that the simultaneous addition of glycerol and hydrophilic polymer to phospholipids as hydrating medium does not simply form a coating layer on vesicle surface but a continuous polymer-glycerol network which, avoiding changes on lamellar assembling, allows small but substantial modifications on dispersion architecture resulting in stable and *in vivo* performing phospholipid vesicles. Their safe composition, easy, biocompatible, environmentally-friendly preparation and the high delivery properties make them as potential carriers to improve local pulmonary activity of curcumin or other compounds that exhibit poor water solubility and low bioavailability. Actually, polymer-glycerosomes thanks to their aptitude to be aerosolized, their selectively deposition in the lung tissue and their simultaneous ability to improve the curcumin antioxidant and anti-inflammatory activity represents promising lung delivery systems which can improve patient compliance and prevent hepatic first-pass metabolism of drug. Additionally, HY-glycerosomes will be test as specific delivery system for tissues, such tumors, which overexpress hyaluronic acid cell surface receptors, CD44.

5. Materials and methods

5.1. Materials

Phospholipon®90G (P90G), a commercial mixture, containing the soy phosphatidylcholine, phosphatidylethanolamine, fatty acids and triglycerides, was kindly supplied by AVG S.r.l. (Garbagnate Milanese, Italy). Sodium hyaluronate low molecular weight (200-400 kDa), was purchased from DSM Nutritional Products AG Branch Pentapharm (Aesch/Switzerland). Curcumin, chitosan (low molecular weight 50-190 KDa and 75-85% deacetylated), sodium iodide, methyl

iodide, N-methylpyrrolidinone, acetone, glycerol and all the other products, of analytical grade, were purchased from Sigma-Aldrich (Milan, Italy). All the cell culture reagents were purchased from Life Technologies Europe (Monza, Italy).

5.2. Preparation and characterization of trimethyl chitosan chloride

The synthesis of trimethyl chitosan reported by Wang *et al.* [43] was slightly modified. Chitosan, sodium iodide and N-methyl pyrrolidinone were vigorously stirred at 60°C for 20 minutes. NaOH solution (11 ml, 15% w/w) and methyl iodide (12 ml) were added, the mixture was maintained for 60 minutes under vigorous stirring at 60°C, and then collected to a refrigerator to avoid the CH_3I evaporation. To control the chitosan degree of quaternization, methyl iodide (5 ml) and NaOH (10 ml, 15% w/w) were added again. The mixture was kept at 60°C for 6 hours and then at room temperature overnight under stirring. The mixture was concentrated, purified by dialysis, treated with a NaCl solution (10% w/w) at 25°C overnight, to change the I-counterions with Cl-counterions, and then freeze-dried. ^{1}H-NMR spectroscopy was performed on a Varian INOVA-500. The ^{1}H-NMR spectra were recorded at 27°C, using deuterium oxide as solvent. All measurements were done with water suppression. The trimethyl chitosan degree of quaternization (DQ%) was calculated using the equation 1 [44]:

$$DQ\% = \left(\frac{[N(CH3)3]}{[H1]} \; x \; \frac{1}{9}\right) x \; 100 \quad \text{eq. 1}$$

Where $[N(CH3)3]$[$N(CH_3)^3$] is the integral of the trimethyl amino group and H^1 is the integral of the proton on the C^1 of the glycoside ring.

5.3. Vesicle preparation

To obtain glycerosomes, curcumin (2 mg/ml) was dispersed in a mixture of glycerol/water (1/1 v/v) and to obtain HY-glycerosomes and TMC-glycerosomes, the same amount of drug was dispersed in a mixture of glycerol/water (1/1 v/v) containing 0.1% (w/v) of sodium hyaluronate or trimethyl chitosan. The dispersions were stirred for 5 h and used to hydrate phospholipids (180 mg/ml) overnight [19,35]. Finally, dispersions were sonicated with a high intensity ultrasonic disintegrator

(Soniprep 150, MSECrowley, London, United Kingdom), for 25, 10, 15 and 25 cycles (2 seconds on and 2 seconds off, 15 μm of probe amplitude) waiting 2 min between each cycle group to promote the cooling of the sample. The schematic illustration of glycerosomes and polymer-glycerosomes is reported in Figure 7.

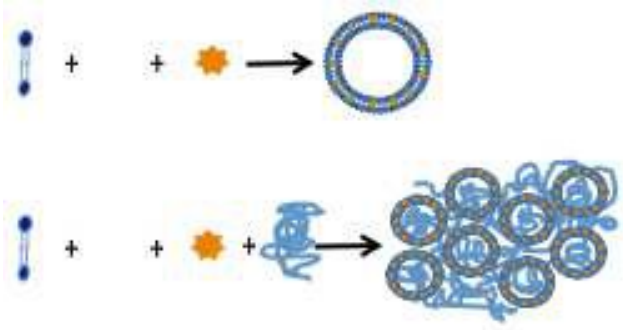

Samples (2 ml) were purified from the non-incorporated drug by dialysis against glycerol/water (2 L) using dialysis tubing (Spectra/Por® membranes: 12–14 kDa MW cut-off, 3 nm pore size; Spectrum Laboratories Inc., DG Breda, The Netherlands) at room temperature for 4 hours, by replacing the water every hour. The water (8 litter total) was enough to theoretically remove all the drug contained in 2 ml of dispersion (4 mg).

5.4. Vesicle characterization

Morphology of each formulation was checked by cryo-TEM (CCiT, University of Barcelona, Spain). A thin aqueous film was formed on a glow-discharged holey carbon grid. The films were vitrified by plunging the grid (kept at 100% humidity and room temperature) into ethane and maintained at its melting point, using a Vitrobot (FEI Company, Eindhoven, The Netherlands). The vitreous films were transferred to a Tecnai F20 TEM (FEI Company), and the samples were observed in a low dose mode. Images were acquired at 200 kV at a temperature between -170 and -175°C, using low-dose imaging conditions with a CCD Eagle camera (FEI Company) [20].

Size distribution (average diameter and polydispersity index, P.I.) and zeta potential of the samples were measured using a Zetasizer nano (Malvern Instrument, London, United Kingdom) after their dilution with the glycerol/water solution.

Entrapment efficiency (EE%) was expressed as the percentage of the amount of incorporated curcumin versus that initially used. Drug amount was determined by HPLC, after dilution of the sample with methanol (1/100) using a chromatograph Alliance 2690 (Waters, Milano, Italy) equipped with a photodiode array detector and a computer integrating apparatus (Empower^{TM} 3). The column was a SunFire C18 (3.5 μm, 4.6×150 mm). The mobile phase was a mixture of acetonitrile, water and acetic acid (95:4.84:0.16, v/v), delivered at a flow rate of 0.7 ml/min. Curcumin content was quantified at 424 nm.

Quantitative determination of phospholipids was carried out using the Stewart assay [45]. Vesicle dispersions (10 μl) were added to the reagent and the obtained solutions were maintained in the dark at room temperature for 30 min and then analysed at 485 nm using a UV spectrophotometer (Spectrometer Lamba 25, Perkin Elmer, Milan, Italy). Aggregation efficiency (AE%) was calculated as the percentage of the P90G amount after dialysis (aggregated) against that initially used.

5.5. Small-Angle X-ray Scattering

Vesicle structure was studied by Small-Angle X-ray Scattering (SAXS). Analysis was recorded at 25°C using a S3-MICRO SAXS camera system (HECUS X-ray Systems, Graz, Austria). The working q-range was 0.003–0.6 $Å^{-1}$, where $q = (4\pi \sin \theta)/\lambda$ is the modulus of the scattering wave vector, θ is the scattering angle and λ is the wavelength. All scattering curves were reproduced three times and a representative curve was selected, plotting the scattering intensity (I) as a function of the scattering vector (q). SAXS patterns were analysed using the GAP (Global Analysis Program) software developed by Pabst [33]. The GAP allows fitting the SAXS pattern of bilayer-based structures, i.e. vesicles and lamellar phases.

5.6. Nebulization and aerodynamic behaviour of vesicular formulations

A Pari SX® air jet nebulizer was used and connected to the Next Generation Impactor^{TM} (NGI, Eur. Ph 7.2, Copley Scientific Ltd., Nottingham, United Kingdom). Samples (3 ml) were placed in the nebulizer and aerosolized for 15 min at 15 l/min. [46]. At the end of each experiment, the sample

deposited in each single stage of the impactor and that undelivered was collected in glass vials using methanol and, the curcumin amount, was analyzed by HPLC. The Emitted Dose (ED%) was calculated as the percentage of drug recovered in the NGI versus the amount of drug placed in the nebulizer. The Fine Particle Dose (FPD) was calculated as the amount of curcumin contained in droplets with size ≤5 μm and the Fine Particle Fraction (FPF), as the ratio of FPD to the total recovered dose. The total amount of curcumin recovered from the impactor was calculated as the sum of all recovered drug. The cumulative amount of curcumin-containing particles with a diameter lower than the stated size of each stage was plotted as a percentage of recovered drug versus the cut-off diameter. Mass median aerodynamic diameter (MMAD) of the particles was extrapolated from the graph (Eur. Ph. 7.2). MMAD and geometric standard deviation (GSD) values were calculated without including the mass deposited in the induction port because of the unavailability of a precise upper size limit for particles deposited in this section [47]. The size and size distribution of vesicles deposited in each stage of the impactor were measured.

5.7. *In vitro* cytotoxicity studies (MTT Assay)

Human basal epithelial alveolar cells (A549) were grown in Dulbecco's Modified Eagle Medium containing l-glutamine, supplemented with 10% foetal bovine serum, 1% penicillin/streptomycin and 1% fungizone, at 37°C, 5% CO_2 and 100% humidity. Before the experiment, A549 cells were placed into 96-well plates at a density of 7.5×10^3 cells/well. After 24 h, cells were treated with curcumin (40, 20, 10, 4, 2 μg/ml) in dispersion or loaded in vesicles. Cells viability was evaluated after 48 h experiment by MTT test. The reagent [3(4,5-dimethylthiazol-2-yl)-2,5-diphenyltetrazolium bromide] (0.5 mg/ml) was added to each well and after 2/3 h the formed crystals were dissolved with dimethyl sulfoxide. The sample intensity was measured spectrophotometrically at 570 nm with a microplate reader (Synergy 4, Reader BioTek Instruments, Bernareggio, Italy) [18]. All experiments were repeated at least three times and in triplicate. Results were expressed as percentage of cell viability in comparison with non-treated control cells (100% viability).

5.8. Effect of curcumin formulations on cell oxidative stress damage

A549 cells were seeded in 96 well plates and incubated at 37°C in 5% CO_2 until confluence was reached [48]. Cells were treated with H_2O_2 (1:30000 dilution) and curcumin in dispersion or loaded in vesicles (20 μg/ml), incubated for 6 hours and then washed with PBS. Untreated cells were used as control (100% viability) while cells treated with H_2O_2 only, were the positive control. The MTT assay was used to assess the protective effect of curcumin on cell damage and death [20].

5.9. *In vitro* inhibition of cytokines by curcumin formulations

The ability of curcumin to inhibit the release of proinflammatory cytokines IL-6 and IL-8 was measured. A549 cells (micoplasma free) were seeded in 96 well plates (10^5cells/well) and incubated at 37°C in 5% CO_2. After 24 h, curcumin loaded vesicles (10 μg/ml) were added and cells were incubated for 4 days. To inhibit the protein secretion, 18 h before the test, the protein transport inhibitor cocktail (eBiosciences, San Diego, CA, USA) was added. At the end of the experiment, cells were fixed with paraformaldehyde (3% in PBS) for 15 min at 25°C, washed two times with foetal calf serum (FCS, 0.5% in PBS) at 4°C, permeabilized with triton (0.3% in PBS) and stained with the anti-cytokine antibodies (anti human IL-8 and IL-6, Biolegend, London, UK) conjugated with fluorescein (FITC). Cell analysis was carried out by Facscalibur (Becton Dickinson, Milan, Italy) using a CellQuest software package (Becton Dickinson, Milan, Italy). For all samples, 20,000 events were acquired in the R1 region gate, which was defined based on forward and side light scatter properties to exclude debris.

5.10. *In vivo* curcumin deposition in the lungs

Male Wistar rats, 2-3 months old and weighing 280-310 g, were obtained from the animal facilities of Faculty of Pharmacy, University of Valencia. They were kept at temperature of 23±1ºC, humidity of 60%, light-dark cycles of 12 hours, fed a standard diet and had *ad libitum* access to water. The protocol for the study was approved by the Animal Care Committee (protocol A1352991914316) of the Faculty of Pharmacy at the University of Valencia, Spain.

Rats were cannulated in the jugular vein to facilitate blood sample collection using a procedure reported previously [49]. Each curcumin formulation was diluted 1:1 in water and 100 μl of obtained dispersion (0.10 μg) was intratracheally administered to each rat (6 animals for group) under isoflurane anaesthesia. Blood samples (200 μl) were taken with heparinized syringes connected to the jugular vein cannula at 0.5, 1, 2, 3, 4, 6, 8, and 24 h after dosing. Samples were centrifuged at 1500 *g* for 5 min and the supernatant plasma was stored at −20°C until analysis. At 24 h, rats were sacrificed and liver, lungs and trachea were excised. Curcumin fluorescence (excitation at 410 nm and emission at 535 nm) was observed using the In-Vivo FX PRO Imaging System (Bruker BioSpin, Barcelona, Spain).

The curcumin concentration in plasma and tissue samples was determined by HPLC. Previously to the injection plasma samples were deproteinized with acetonitrile while tissue samples were homogenized in a mixture of water and acetonitrile (30:70, v/v) using a Ultra-Turrax®T25 homogenizer (IKA®Werke GmbH & Co, Staufen, Germany) and centrifuged at 12500 *g* for 15 min. The left inferior lobe, right inferior lobe, right superior lobe and the rest of the whole lungs were separately treated and analysed at 425 nm, using a chromatograph Thermo Scientific (Madrid, Spain), a Novapak C18 column (Waters, Madrid, Spain) and a mobile phase of water/acetonitrile/acetic acid (24:75:1, v/v/v) delivered at a flow rate of 1 ml/min.

5.11. Statistical analysis of data

Results are expressed as the mean ± standard deviation and significance was tested at the 0.05 level of probability (p). Analysis of variance (ANOVA) was used to substantiate statistical differences between groups while Student's t-test was used for comparison between two samples using XLStatistic for Excel. The multiple comparisons of in vivo results were performed by the Scheffe or Dunnet tests using IBM SPSS statistics for Windows.

Acknowledgments

This work was partially supported by grants from MIUR (PRIN 2010-2011, Prot. 2010H834LS_004).

Bibliography.

[1] J. B. Calixto, M. F. Otuki, A. R. S. Santos, *Planta Med.* **2003**, *69*, 973.

[2] J. B. Calixto, M. M. Campos, M. F. Otuki, A. R. Santos, *Planta Med.* **2004**, *70*, 93.

[3] X. Hu, F.-F. Yang, L.-H. Quan, C.-Y. Liu, X.-M. Liu, C. Ehrhardt, Y.-H. Liao, *Eur. J. Pharm. Biopharm.* **2014**, *88*, 1064.

[4] M. Masuda, N. Suzuki, S. Taniguchi, T. Oikawa, T. Nonaka, T. Iwatsubo, S. Hisanaga, M. Goedert, M. Hasegawa, *Biochemistry* **2006**, *45*, 6085.

[5] M. E. Egan, M. Pearson, S. A. Weiner, V. Rajendran, D. Rubin, J. Glöckner-Pagel, S. Canny, K. Du, G. L. Lukacs, M. J. Caplan, *Science* **2004**, *304*, 600.

[6] K. G. Ramawat, Ed. , *Herbal Drugs: Ethnomedicine to Modern Medicine*, Springer Berlin Heidelberg, Berlin, Heidelberg, **2009**.

[7] M. T. Huang, H. L. Newmark, K. Frenkel, *J. Cell. Biochem. Suppl.* **1997**, *27*, 26.

[8] M. L. Manca, I. Castangia, M. Zaru, A. Nácher, D. Valenti, X. Fernàndez-Busquets, A. M. Fadda, M. Manconi, *Biomaterials* **2015**, *71*, 100.

[9] K. K. Chereddy, R. Coco, P. B. Memvanga, B. Ucakar, A. des Rieux, G. Vandermeulen, V. Préat, *J. Control. Release* **2013**, *171*, 208.

[10] M. Salahshoor, S. Mohamadian, S. Kakabaraei, S. Roshankhah, C. Jalili, *J. Tradit. Complement. Med.* **2015**, DOI 10.1016/j.jtcme.2014.11.034.

[11] Q. Yao, Y. Lin, X. Li, X. Shen, J. Wang, C. Tu, *Toxicol. Lett.* **2013**, *222*, 72.

[12] C. Mohanty, M. Das, S. K. Sahoo, *Mol. Pharm.* **2012**, *9*, 2801.

[13] O. Naksuriya, S. Okonogi, R. M. Schiffelers, W. E. Hennink, *Biomaterials* **2014**, *35*, 3365.

[14] M. Zaru, C. Sinico, A. De Logu, C. Caddeo, F. Lai, M. L. Manca, A. M. Fadda, *J. Liposome Res.* **2009**, *19*, 68.

[15] M. Zaru, S. Mourtas, P. Klepetsanis, A. M. Fadda, S. G. Antimisiaris, *Eur. J. Pharm. Biopharm.* **2007**, *67*, 655.

[16] Q. T. Zhou, S. S. Y. Leung, P. Tang, T. Parumasivam, Z. H. Loh, H.-K. Chan, *Adv. Drug Deliv. Rev.* **2015**, *85*, 83.

[17] Z. Liang, R. Ni, J. Zhou, S. Mao, *Drug Discov. Today* **2014**, DOI 10.1016/j.drudis.2014.09.020.

[18] M. L. Manca, C. Sinico, A. M. Maccioni, O. Diez, A. M. Fadda, M. Manconi, *Pharmaceutics* **2012**, *4*, 590.

[19] M. L. Manca, M. Zaru, M. Manconi, F. Lai, D. Valenti, C. Sinico, A. M. Fadda, *Int. J. Pharm.* **2013**, *455*, 66.

[20] M. L. Manca, I. Castangia, C. Caddeo, D. Pando, E. Escribano, D. Valenti, S. Lampis, M. Zaru, A. M. Fadda, M. Manconi, *Colloids Surf. B. Biointerfaces* **2014**, *123*, 566.

[21] A. J. Bollet, W. M. Bonner, J. L. Nance, *J. Biol. Chem.* **1963**, *238*, 3522.

[22] B. T. Shannon, S. H. Love, *Immunol. Commun.* **1980**, *9*, 735.

[23] Z. Darzynkiewicz, E. A. Balazs, *Exp. Cell Res.* **1971**, *66*, 113.

[24] K. Pritchard, A. B. Lansley, G. P. Martin, M. Helliwell, C. Marriott, L. M. Benedetti, *Int. J. Pharm.* **1996**, *129*, 137.

[25] S. T. Lim, G. P. Martin, D. J. Berry, M. B. Brown, *J. Control. Release* **2000**, *66*, 281.

[26] S. Arpicco, C. Lerda, E. Dalla Pozza, C. Costanzo, N. Tsapis, B. Stella, M. Donadelli, I. Dando, E. Fattal, L. Cattel, M. Palmieri, *Eur. J. Pharm. Biopharm.* **2013**, *85*, 373.

[27] S. Barbault-Foucher, R. Gref, P. Russo, J. Guechot, A. Bochot, *J. Control. Release* **2002**, *83*, 365.

[28] F. Andrade, D. Rafael, M. Videira, D. Ferreira, A. Sosnik, B. Sarmento, *Adv. Drug Deliv. Rev.* **2013**, *65*, 1816.

[29] M. Rinaudo, *Prog. Polym. Sci.* **2006**, *31*, 603.

[30] S. M. van der Merwe, J. C. Verhoef, J. H. M. Verheijden, A. F. Kotzé, H. E. Junginger, *Eur. J. Pharm. Biopharm.* **2004**, *58*, 225.

[31] V. K. Mourya, N. N. Inamdar, *J. Mater. Sci. Mater. Med.* **2009**, *20*, 1057.

[32] J. Li, I. W. Lee, G. H. Shin, X. Chen, H. J. Park, *Eur. J. Pharm. Biopharm. Off. J. Arbeitsgemeinschaft für Pharm. Verfahrenstechnik e.V* **2015**, *94*, 322.

[33] G. Pabst, M. Rappolt, H. Amenitsch, P. Laggner, *Phys. Rev. E* **2000**, *62*, 4000.

[34] M. Zaru, M. L. Manca, A. M. Fadda, G. Orsini, *Glycerosomes and Use Thereof in Pharmaceutical and Cosmetic Preparations for Topical Applications*, **2012**.

[35] M. L. Manca, M. Manconi, M. Zaru, I. Castangia, A. Cabras, N. Cappai, A. M. Fadda, *Ialurosomi, Loro Uso in Composizioni Topiche Farmaceutiche O Cosmetiche E Relativo Procedimento Di Preparazione*, **2014**, RM2014A000687.

[36] A. Jintapattanakit, S. Mao, T. Kissel, V. B. Junyaprasert, *Eur. J. Pharm. Biopharm.* **2008**, *70*, 563.

[37] S.-N. Park, H. J. Lee, K. H. Lee, H. Suh, *Biomaterials* **2003**, *24*, 1631.

[38] S. Ganesan, A. N. Faris, A. T. Comstock, S. S. Chattoraj, A. Chattoraj, J. R. Burgess, J. L. Curtis, F. J. Martinez, S. Zick, M. B. Hershenson, U. S. Sajjan, *Respir. Res.* **2010**, *11*, 131.

[39] R. Motterlini, R. Foresti, R. Bassi, C. J. Green, *Free Radic. Biol. Med.* **2000**, *28*, 1303.

[40] G. C. Jagetia, B. B. Aggarwal, *J. Clin. Immunol.* **2007**, *27*, 19.

[41] R. Abu-Dahab, U. F. Schäfer, C.-M. Lehr, *Eur. J. Pharm. Sci.* **2001**, *14*, 37.

[42] M. V Suresh, M. C. Wagner, G. R. Rosania, K. A. Stringer, K. A. Min, L. Risler, D. D. Shen, G. E. Georges, A. T. Reddy, J. Parkkinen, R. C. Reddy, *Am. J. Respir. Cell Mol. Biol.* **2012**, *47*, 280.

[43] S. Wang, T. Jiang, M. Ma, Y. Hu, J. Zhang, *Int. J. Pharm.* **2010**, *386*, 249.

[44] R. J. Verheul, M. Amidi, S. van der Wal, E. van Riet, W. Jiskoot, W. E. Hennink, *Biomaterials* **2008**, *29*, 3642.

[45] J. C. M. Stewart, *Anal. Biochem.* **1980**, *104*, 10.

[46] V. A. Marple, B. A. Olson, K. Santhanakrishnan, D. L. Roberts, J. P. Mitchell, B. L. Hudson-Curtis, *J. Aerosol Med.* **2004**, *17*, 335.

[47] M. Taki, C. Marriott, X.-M. Zeng, G. P. Martin, *Int. J. Pharm.* **2010**, *388*, 40.

[48] M. L. Manca, M. Manconi, A. M. Falchi, I. Castangia, D. Valenti, S. Lampis, A. M. Fadda, *Colloids Surfaces B Biointerfaces* **2013**, *111*, 609.

[49] F. Torres-Molina, J. C. Aristorena, C. Garcia-Carbonell, L. Granero, J. Chesa-Jiménez, J. Pla-Delfina, J. E. Peris-Ribera, *Pharm. Res.* **1992**, *9*, 1587.

Figure Captions

Figure 1. Macroscopic appearance and Cryo-TEM micrographs of the curcumin loaded glycerosomes (A), HY-glycerosomes (B), and TMC-glycerosomes (C).

Figure 2. Mean diameter (A), zeta potential (B) and entrapment efficiency (C) of glycerosomes, HY-glycerosomes and TMC-glycerosomes during 90 days of storage at room temperature (25±1°C). Bars represent standard deviation obtained from 3 samples.

Figure 3. Representative SAXS diffraction profiles (A) of curcumin loaded glycerosome, HY-glycerosomes and TMC-glycerosomes and calculated bilayer values (B). d_B: bilayer thickness, z_H: distance of head group from the centre of the bilayer, σ_H: polar head amplitude. Values represent mean ± standard deviation (n = 3).

Figure 4. Percentage of curcumin deposited in the different impactor stages (A) and mean diameter (B) of glycerosomes, HY-glycerosomes and TMC-glycerosomes measured before (BN) and after nebulization. Values represent mean ± standard deviation (n = 3).

Figure 5. In vitro A549 cell bioavailability after 48 h of incubation with curcumin in dispersion or loaded in glycerosomes, HY-glycerosomes and TMC-glycerosomes at different dilutions (2, 4, 10, 20, 40 μg/ml of curcumin) (A). Protective effect of curcumin dispersion and vesicles against H_2O_2-induced oxidative stress in A549 cells at 6 h (B). Inhibition percentage of IL-6 and IL-8 on A549 cells treated with curcumin loaded vesicles (C). Data are reported as mean values±standard deviation. The same symbols indicate values statistical equivalents ($p>0.05$). All symbols indicate statistical differences with respect to curcumin dispersion. In panel B, symbol ° indicates statistical differences with respect to curcumin dispersion and H_2O_2 and * indicates statistical differences with respect to H_2O_2

Figure 6. Curcumin deposited in the different parts of the respiratory tree (A) and curcumin fluorescence distribution in lungs and liver excised from rats 24 h after the intratracheal administration of the different formulations (B). Data are reported as mean values ± standard deviation. The same symbols indicate values statistical equivalents ($p>0.05$). All symbols indicate statistical differences with respect to curcumin dispersion.

Figure 7. Schematic illustration of the structure of glycerosomes and polymer-glycerosomes.

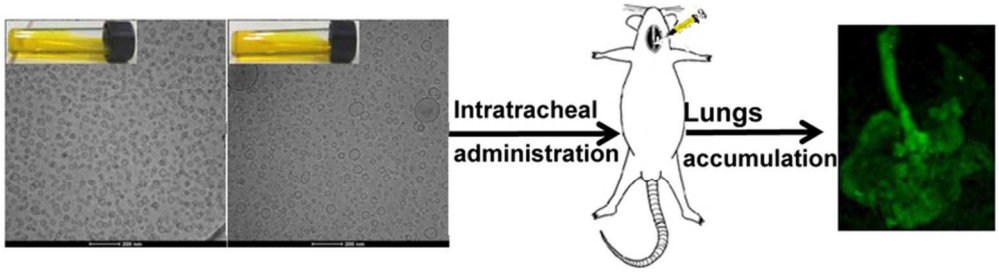

35x9mm (600 x 600 DPI)